

It is noted here, that the other two boundary conditions at  $r = 0$  are of the form

$$\lim_{r \rightarrow 0} (r W_{,rr} + \mu^2 W_{,r}) = 0 \quad \text{or} \quad W_{,r} = 0 \quad (2a)$$

$$\lim_{r \rightarrow 0} (r W_{,rrr} + W_{,rr} - \frac{\phi^2}{r} W_{,r}) = 0 \quad \text{or} \quad W = 0 \quad (2b)$$

Simplifying Eq. (2b) by introducing the result from Eq. (3a) following and using L'Hospital's rule, the boundary conditions reduce to

$$W_{,r} = 0 \quad \text{or} \quad W_{,r} = 0 \quad (3a)$$

$$W_{,rr} (1 - \phi^2) = 0 \quad \text{or} \quad W = 0 \quad (3b)$$

For the axisymmetric problem which is considered here, Eq. (3a) is automatically satisfied. From Eq. (3b), since  $W \neq 0$ , it is noted that the only boundary condition left is

$$(1 - \phi^2) W_{,rr} = 0 \quad \text{at} \quad r = 0 \quad (4)$$

and that is satisfied automatically for the isotropic case.

Since at  $r = 0$ ,  $W_{,rr} \neq 0$ , Eq. (4) is satisfied only if  $\phi^2 = 1$  at the origin. In fact the concept of polar orthotropy cannot be strictly enforced up to the origin which is a singular point. A satisfactory physical explanation is that the radial fibers converging to a point cannot have any cross-sectional area of its own at that point thus leading to isotropic behavior at the origin. It is believed here that this violation of boundary condition leads to erroneous results in certain formulations where differential equations of equilibrium are dealt with as in the case of Galerkin method, but are probably eliminated while dealing with energies in the average sense as in the Lagrangian approach.

### III. Examples and Results

The present problem is solved using one term and two term mode-shapes using both the Lagrangian and Galerkin methods, and the results are compared with those available in the literature. The assumed mode shapes are.

$$A_1 (1 - \frac{r^2}{a^2})^2$$

and

$$A_1 (1 - \frac{r^2}{a^2})^2 + A_2 (1 - \frac{r^2}{a^2})^3$$

These mode-shapes satisfy the boundary conditions given by Eqs. (1) and (3a) and do not satisfy Eq. (4) except when  $\phi^2 = 1$ . The results of the present analysis are tabulated in Table 1. When  $\phi^2 = 1$  (isotropic case), the Galerkin and Lagrangian solutions are identical, as is to be expected because all the boundary conditions are satisfied. The two-term solution in this case is  $\lambda = 10.22$ , and this compares excellently with the value of  $\lambda = 10.2158$  as given in Ref. 4. However, in the Galerkin method, the frequency decrease with increase in the value of  $\phi^2$  like those given in Ref. 3. The two-term solution with the Lagrangian approach gives good agreement with those in Ref. 1. The frequency equation for this case is

$$\lambda^4 - (1704 + \frac{1272}{5} \phi^2) \lambda^2 + (115920 + 74592 \phi^2 + 3024 \phi^4) = 0$$

To test the argument that it is the nonsatisfaction of Eq. (4) that leads to these erroneous results, a hypothetical problem where the plate is constrained to have  $W_{,rr} = 0$  at the origin was examined. Equation (4) is now satisfied, and the solutions

Table 1 Comparison of nondimensional frequency ( $\lambda$ ) values

$\phi^2$	Present investigation				Ref. 1	Ref. 3
	Lagrangian method	Galerkin method	One term	Two term		
0	8.95	8.42	10.96	11.05	7.16	10.61
1	10.33	10.22	10.33	10.22	10.22	9.8
4	13.66	13.47	8.16	7.56	13.29	7.25
9	17.89	16.69	0	0	16.37	0

obtained by the Lagrangian and Galerkin approaches for an assumed mode shape  $W = A_1 (1 - 4(r^3/a^3) + 3(r^4/a^4))$  were identical, and the resulting frequency is  $\lambda^2 = 18(6 + \phi^2)$ .

### IV. Conclusions

The Galerkin and Lagrangian methods of solution give identical results provided the assumed mode-shape satisfies all the boundary conditions obtained from the variational principle. The present analysis shows that the singularity at the origin due to the assumption of general orthotropy,  $\phi^2 \neq 1$ , could have considerable effect on the results in certain approaches, giving qualitatively erroneous results. However, the Lagrangian approach shows to preserve the behavior qualitatively and gives reasonably good quantitative results as shown here. This is true even though the assumed mode-shape does not satisfy all the boundary conditions arising from the variational principle. It is also expected that in the bending, buckling, and the large deflection analysis of orthotropic circular plates, the Galerkin method will lead to results which are in error qualitatively.

### References

- 1 Akasaka, T. and Takagishi, T., "Vibration of Corrugated Diaphragm," *JSME Bulletin*, Vol. 1, No. 3, 1958, pp. 215-221.
- 2 Borsuk, K., "Free Vibration of Rotations of a Cylindrically Orthotropic Circular Plate," *Archiwum Mechaniki Stosowanej*, Vol. 12, No. 5/6, 1960, pp. 649-665.
- 3 Pandalai, K. A. V. and Patel, S. A., "Natural Frequencies of Orthotropic Circular Plate," *AIAA Journal*, Vol. 3, April 1965, pp. 780-781.
- 4 Leissa, A. W., "Vibration of Plates," NASA SP-160.

## Effects of Atomic Oxygen on Graphite Ablation

Chul Park\*

NASA Ames Research Center,  
Moffett Field, Calif.

METZER et al.<sup>1</sup> derived a semiempirical formula to describe the observed ablation rates of commercial grade (i.e., isotropic) graphites in the form

$$\dot{m}(R/p)^{1/2} = 1.19 \times 10^6 e^{-22,140/T_w} \{ 30.5/R + 4.85 \times 10^{15} \times [e^{-22,140/T_w} / (1 + 1.6 \times 10^7 p^{-2/3} e^{-61,700/T_w})]^2 \}^{-1/2} \quad (1)$$

where  $\dot{m}$ ,  $R$ ,  $p$ , and  $T_w$  are mass loss rate in  $\text{gcm}^{-2} \text{sec}^{-1}$ , nose radius in cm, stagnation-point pressure in atm, and wall temperature in K, respectively. The purpose of the present

Received March 29, 1976; revision received June 28, 1976.

Index categories: Material Ablation; Boundary Layers and Convective Heat Transfer—Laminar; Thermochemistry and Chemical Kinetics.

\*Research Scientist. Member AIAA.

Note is to point out that the formula is inapplicable to low-density flows containing dissociated oxygen. In the low-density regimes, the following chemical reactions occur at the surface:<sup>2-8</sup> 1)  $C(c) + O_2 \rightarrow CO + O - 1.40$  eV (endothermic) with reaction probability  $\epsilon_1$ ; 2)  $C(c) + O \rightarrow CO + 3.76$  eV (exothermic), with  $\epsilon_2$ ; and 3)  $C(c) + O + O \rightarrow C(c) + O_2 + 5.08$  eV (exothermic), with  $\epsilon_3$ . Reactions forming  $CO_2$  and those between nitrogen species and graphite are neglected since they are comparatively slower.<sup>2-6</sup>

Experimental results<sup>3-5,7,8,10-16</sup> on  $\epsilon_1$  from the tests on isotropic graphites (vs pyrolytic graphites) are summarized in Fig. 1. The data of Olander et al.<sup>3,4</sup> for two crystallographic planes of pyrolytic graphite are included because the average of the values of  $\epsilon_1$  for the two crystallographic planes is expected to be comparable to the value for the isotropic polycrystalline graphite. Except for the data by Rosner and Allendorf,<sup>7,8</sup> which deviate from the rest for an unknown reason, this group of graphites exhibits fairly consistent reaction characteristics. In the present work, therefore, only this group of materials is considered for the analysis. The choice is made because a) these materials have been tested extensively, b) they exhibit consistent reaction characteristics, and c) Eq. (1), with which the present analysis is to be compared, also is based on the data for these materials.

Figure 1 also shows the analytical expressions for the material derived in Refs. 1 and 9, both normalized at 1 atm where they are expected to be most accurate. In the present work, an arbitrary third expression

$$\epsilon_1 = [1.43 \times 10^{-3} + 0.01e^{-1450/T_w}] / [1 + 2 \times 10^{-4}e^{13,000/T_w}] \quad (2)$$

is used to represent the isographite data. As seen in the figure, the present formula approximates the experimental data more closely than either of the two previous expressions.

In Fig. 2 the existing data<sup>2,5,7,8,17-19</sup> for atomic oxygen are shown for both pyrographites and isographites. As seen here, the two types exhibit nearly the same reaction characteristics. The data are approximated here by

$$\epsilon_2 = 0.63e^{-1160/T_w} \quad (3)$$

The probability  $\epsilon_3$  is found by Berkowitz-Mattuck<sup>2</sup> to be

$$\epsilon_3 \cong \epsilon_2 \quad (4)$$

for  $1500 < T_w < 2500$  K. In the absence of any other data, Eq. (4) is used over the entire temperature range in the present work.

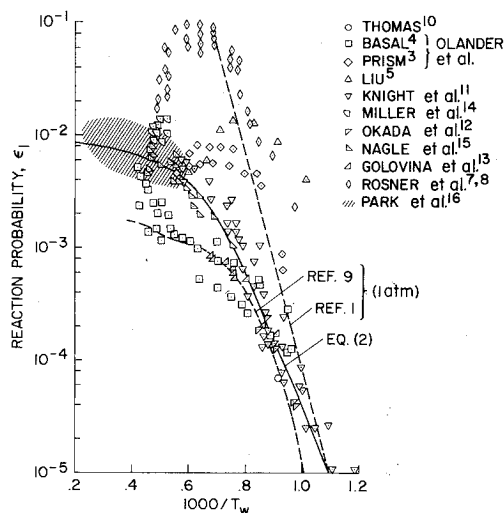


Fig. 1 Reaction probability of isotropic graphites to molecular oxygen,  $\epsilon_1$ .

Using the above model, the boundary-layer equations were solved to obtain heat-transfer rates. Air was assumed to reach equilibrium at the edge of the stagnation-point boundary layer, and to be frozen within the boundary layer.<sup>20</sup> Viscosity was approximated by  $\mu = 6.27 \times 10^{-4}(T/2000)^{0.75}$  poise, and the Prandtl and Schmidt numbers were taken to be 0.7 and 0.5, respectively. Ionization energy was treated as a component of thermal energy.<sup>21</sup> The heat-transfer rate was equated to the radiated power in determining the wall temperature. Emissivity of graphite was assumed to be 0.9. Blowing effect was small, and hence was accounted for using a linear blowing-effect model, the coefficient for which was derived by the author through numerical solution of governing differential equations for conditions appropriate to the

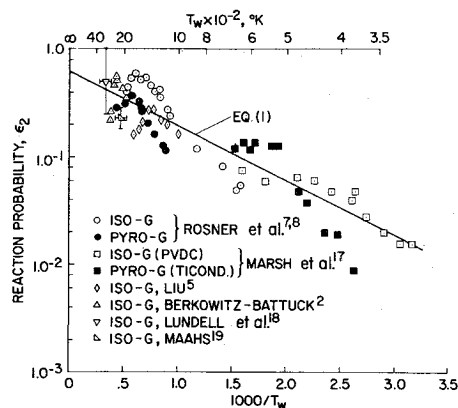


Fig. 2 Reaction probability of graphitic materials to atomic oxygen,  $\epsilon_2$ .

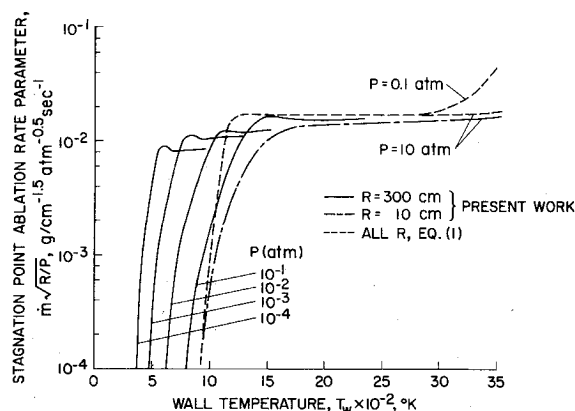


Fig. 3 Stagnation-point ablation rates calculated by the present method vs calculations by Eq. (1).

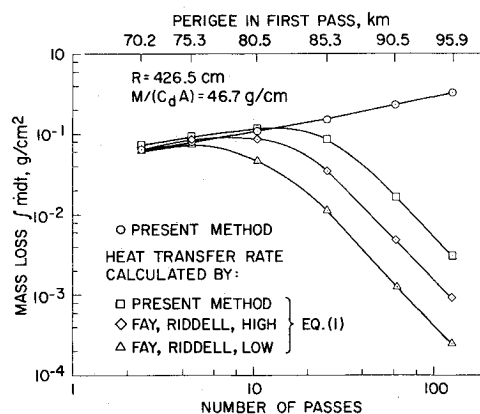


Fig. 4 Integrated mass loss calculated by the present method vs calculations by Eq. (1) for a skipping trajectory for transfer from geosynchronous to space shuttle orbit.

present environments. The calculation procedure is that described in Ref. 20.

In Fig. 3, the ablation rates  $\dot{m}$  obtained by the present method are shown for typical conditions and are compared with those obtained using Eq. (1). As seen in the figure, the present results agree closely with those of Eq. (1) for  $R=10$  cm, except for a narrow temperature range  $1000 < T_w < 1400$  K where the difference in  $\epsilon_1$  values between Eqs. (1) and (2) influences the results. For the low-density, large- $R$  conditions, the present calculations clearly predict greater ablation rates. The increase is because of oxidation by atomic oxygen.

The integrated mass loss  $\int \dot{m} dt$  was calculated for a group of flight trajectories. The trajectories considered start from the geosynchronous orbit and enter the Earth's atmosphere many times in a skipping motion, following near-elliptic, decaying orbits. The calculations were made assuming zero lift and were terminated when the sum of kinetic and potential energies of the vehicle reached that of the space shuttle orbit. The nose radius and the ballistic coefficients were taken<sup>22</sup> to be  $R=426.5$  cm and  $M/C_d A=46.7$  g/cm<sup>2</sup>, corresponding roughly to a truncated hemisphere-cylinder of 426.5-cm radius and 426.5-cm cylinder diameter with 10,000-kg mass and drag coefficient of  $C_d=1.5$ . The orbit calculation was performed under a simplifying assumption that the entries occur only in the Earth's equatorial plane from west to east. The present results are compared in the figure with those calculated by using Eq. (1). In applying Eq. (1), heat-transfer rates and corresponding wall temperatures were calculated by three different methods, i.e., the present model, Fay and Riddell's<sup>23</sup> high-limit value that assumes the chemical energy of dissociation to be transmitted completely into the wall, and the low-limit value that excludes the chemical energy.

As seen in Fig. 4, for the low-perigee, low number-of-pass (i.e., steep) trajectories, the present calculation and those by Eq. (1) are in excellent agreement. The agreement is expected because the flow is in the diffusion-controlled regime where the surface kinetics are immaterial. However, for high-perigee, high number-of-pass (i.e., shallow) trajectories for which surface kinetics are likely to be important, the present calculation yields mass loss values much greater than Eq. (1), i.e., up to three orders of magnitude, depending on the method used for computing the heat-transfer rate. The difference is because of the surface oxidation by atomic oxygen.

## References

- Metzger, J. W., Engel, M. J., and Diaconis, N. S., "Oxidation and Sublimation of Graphite in Simulated Re-entry Environments," *AIAA Journal*, Vol. 5, March 1967, pp. 451-460.
- Berkowitz-Mattuck, J. B., "Research to Determine the Effects of Surface Catalyticity on Materials Behavior in Dissociated Gas Streams—ATJ Graphite," AFML-TR-70-172, Feb. 1970, Arthur D. Little, Inc., Cambridge, Mass.
- Olander, D. R., Siekhaus, W., Jones, R., and Schwarz, J. A., "Reactions of Modulated Molecular Beams with Pyrolytic Graphite. I. Oxidation of the Prism Plane," *Journal of Chemical Physics*, Vol. 57, July 1972, p. 408-420.
- Olander, D. R., Jones, R. H., Schwarz, J. A., and Siekhaus, W. J., "Reactions of Modulated Molecular Beams with Pyrolytic Graphite. II. Oxidation of the Prism Plane," *Journal of Chemical Physics*, Vol. 57, July 1972, pp. 421-433.
- Liu, G.N.K., "High Temperature Oxidation of Graphite by a Dissociated Oxygen Beam," Ph.D. thesis, 1973, Massachusetts Institute of Technology, Dept. of Aeronautics and Astrophysics, Cambridge, Mass.
- McCarroll, B. and McKee, D. W., "The Reactivity of Graphite Surfaces with Atoms and Molecules of Hydrogen, Oxygen, and Nitrogen," *Carbon*, Vol. 9, March 1971, pp. 301-311.
- Rosner, D. E. and Allendorf, H. D., "Kinetics of the Attack of Refractory Materials by Dissociated Gases," *Heterogeneous Kinetics at Elevated Temperatures*, edited by G. R. Belton and W. L. Worrell, Plenum Press, New York, 1970, pp. 231-251.
- Rosner, D. G. and Allendorf, H. D., "Comparative Studies of the Attack of Pyrolytic and Isotropic Graphite by Atomic and Molecular Oxygen at High Temperatures," *AIAA Journal*, Vol. 6, April 1965, pp. 650-654.
- Maahs, H. G., "Oxidation of Carbon at High Temperatures: Reaction-Rate Control or Transport Control," TN D-6310, June 1971, NASA.
- Thomas, J.M., "Microscopic Studies of Graphite Oxidation," *Chemistry and Physics of Carbon*, edited by P. L. Walker, Jr., Vol. 1, Marcel Dekker, New York, 1965, pp. 122-202.
- Knight, D. D. and Knechtel, E. D., "Graphite Oxidation at Low Temperature in Subsonic Air," AIAA Paper 73-735, Palm Springs, Calif., 1973.
- Okada, J. and Ikegawa, T., "Combustion Rate of Artificial Graphites From 700°C to 2000°C in Air," *Journal of Applied Physics*, Vol. 24, Sept. 1953, pp. 1249-1250.
- Golovina, E. S. and Khaustovich, G. P., "The Interaction of Carbon with Carbon Dioxide and Oxygen at Temperatures up to 3000 °K," *Proceedings of the 8th Symposium (International) on Combustion*, Williams and Wilkins, New York, 1952, pp. 784-792.
- Miller, I. R. and Sutton, K., "An Experimental Study of the Oxidation of Graphite in High Temperature Supersonic and Hypersonic Environments," TN D-3344, July 1966, NASA.
- Nagle, J. and Strickland-Constable, F., "Oxidation of Carbon Between 1000-2000°C," *Proceedings of the 5th Carbon Conference*, MacMillan, New York, 1962, pp. 154-164.
- Park, C. and Appleton, J. P., "Shock Tube Measurements of Soot Oxidation Rates," *Combustion and Flame*, Vol. 20, June 1973, pp. 369-379.
- Marsh, H., O'Hair, T. E., and Wynnes-Jones, L., "The Carbon-Atomic Oxygen Reaction Surface-Oxide Formation on Paracrystalline Carbon and Graphite," *Carbon*, Vol. 7, May 1969, pp. 555-566.
- Lundell, J. H. and Dickey, R. R., "Ablation of ATJ Graphite at High Temperatures," *AIAA Journal*, Vol. 11, Feb. 1973, pp. 216-222.
- Maahs, H. G., "A Study of the Effect of Selected Material Properties on the Ablation Performance of Artificial Graphites," TN D-6624, March 1972, NASA.
- Dorrance, W. H., *Viscous Hypersonic Flow*, McGraw-Hill, New York, 1962, pp. 102-143.
- Okuno, A. F. and Park, C., "Stagnation-Point Heat-Transfer Rate in Nitrogen Plasma Flows; Theory and Experiment," *Journal of Heat Transfer, Transactions of ASME*, Ser. C, Vol. 92, Aug. 1970, pp. 372-384.
- Strauss, E. L., "Ablative and Metallic Heat Shields for Aerobraking Reentry," Rept. MCR-72-324, 1972, Martin Marietta Aerospace, Denver, Colo.
- Fay, J. A. and Riddell, F. R., "Theory of Stagnation-Point Heat Transfer in Dissociated Air," *Journal of Aeronautical Sciences*, Vol. 25, Feb. 1958, pp. 73-85.

## Thermocouple Time Constant Measurement by Cross Power Spectra

Warren C. Strahle\* and M. Muthukrishnan†  
Georgia Institute of Technology, Atlanta, Ga.

### Introduction

THE measurement of fluctuating temperatures downstream of the combustor in turbopropulsion systems is required to quantify the importance of entropy noise generation in these systems.<sup>1-3</sup> It is well known, however, that most thermocouples suitable for use in such a hostile environment have response times considerably longer than required for flat response in the audible frequency range. Consequently, they must be compensated. Central to the compensation problem is the problem of measuring the response time of a given thermocouple, because it must be measured in the environment which it will see in use. This is so because the

Received July 19, 1976. This work was supported by NASA under grant no. NSG 3015.

Index categories: Aircraft Noise, Powerplant; Airbreathing Engine Testing; Combustion in Gases.

\*Regents' Professor. Associate Fellow AIAA.

†Graduate Research Assistant.